

# Enhanced Case-II diffusion of diluents into glassy polymers undergoing plastic flow

Q.-Y. Zhou<sup>1</sup>, A.S. Argon<sup>\*</sup>, R.E. Cohen

*Department of Mechanical Engineering, Massachusetts Institute of Technology, Cambridge, MA 02139, USA*

Received 2 February 2000; received in revised form 5 May 2000; accepted 5 May 2000

## Abstract

Dramatic enhancement of diluent conductance in glassy polymers actively undergoing plastic flow has long been suspected. We report observations of this phenomenon in a glassy poly(ether imide) (Ultem)<sup>™</sup> in the presence of resorcinol bis(diphenyl phosphate) (RDP) by means of the limited-supply diffusion experiment developed earlier by Nealey et al. In this experiment it is demonstrated that RDP uptake in plastically deforming Ultem is nearly identical at 113°C, i.e. 102°C below  $T_g$ , as it is at 215°C, at  $T_g$ , without concurrent plastic flow. While the characteristic profiles of penetrating Case-II fronts are present in experiments at 130°C without plastic flow, they are absent in experiments above  $T_g$  without plastic flow and in those at 113°C undergoing concurrent plastic flow. This demonstrates that in the plastically deforming polymer, well below  $T_g$ , a steady dilated flow state exists, which resembles in its molecular level conformational rearrangements that at  $T_g$  without deformation, where in both the resistance to diluent penetration has been radically reduced. Based on the measured diffusion constant of RDP in Ultem, the structural correspondence of the thermally dilated state at  $T_g$  and the flow dilated state at 113°C is equivalent to an increase of the diffusion constant by a factor of  $1.9 \times 10^4$  in the latter. © 2000 Elsevier Science Ltd. All rights reserved.

*Keywords:* Case-II diffusion; Dilated flow states; Plastic-flow enhanced diffusion

## 1. Introduction

The penetration of low molecular weight diluents into glassy polymers presents unique features that have been explored extensively since the early studies of Alfrey et al. [1] who labeled the process as Case-II diffusion, to differentiate it from Fickian (isotope) diffusion, which they labeled as Case-I. Under no externally applied stresses, the diluents penetrate into the glassy polymer in the form of sharp swelling fronts at constant velocity under constant conditions of the given levels of external activity of the diluent and the prevailing temperature, pushing in front Fickian precursors. There are definitive experiments carried out to measure the characteristics of the penetration process of which the most thorough are those of Kramer and co-workers [2,3] involving the sorption of a series of iodoalkanes into polystyrene. There have been many models proposed for the process starting with that of Thomas and Windle [4] followed by many variants, reviewed recently by Argon et al. [5] in connection with a mechanistic model of

the self similar advance of the Case-II sorption fronts as material-misfit-driven elasto-plastic reverse extrusion processes occurring ultimately at a very narrow front.

An important special manifestation of the Case-II diffusion process was encountered in a series of experiments of toughness enhancement by Gebizlioglu et al. [6] in which a small volume concentration of precipitated sub-micron size, low molecular weight polybutadiene (PB) diluent pools were observed to dramatically increase the toughness of polystyrene through enhanced craze plasticity. In an associated theoretical model the toughening effect was attributed to a negative-pressure-induced step-increase of the solubility of the PB in the craze matter tufts, resulting in a sharp increase in plasticization of the PS where the observed kinetics implied a diffusion constant in excess of  $3 \times 10^{-12}$  cm<sup>2</sup>/s at room temperature. The observed enhancement of toughness [7,8] and the separately measured acceleration of craze growth kinetics [9,10] of PS in the presence of low molecular weight PB indicated that the latter must penetrate PS craze matter at 20°C at the same rate as if the PS were at 110°C. Attempts to demonstrate that this accelerated diffusion results from the effect of stresses were unsuccessful in specially designed Case-II sorption experiments of RDP (resorcinol bis diphenyl phosphate) into Ultem (glassy polyether imide) in which the

<sup>\*</sup> Corresponding author. Tel.: +1-617-253-2217; fax: +1-617-258-8742.

*E-mail address:* oona@mit.edu (A.S. Argon).

<sup>1</sup> Present address: Chemical Engineering Department, University of Alabama, Birmingham, AL, USA.

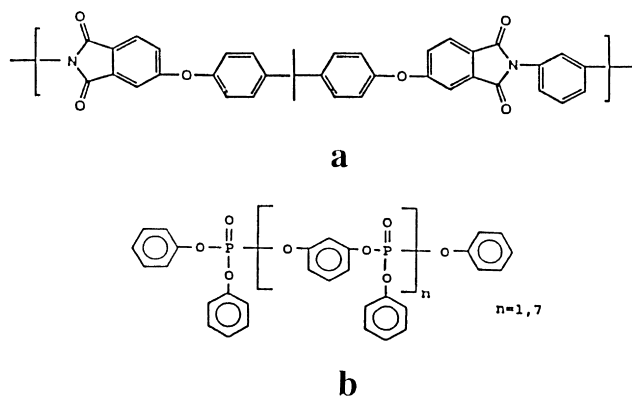


Fig. 1. Chemical Structures of: (a) Ultem; (b) RDP.

surface layers of Ultem were subjected to bi-axial tensile or compressive stresses of up to 60% of the tensile yield strength [11]. While the failure of this experiment could be attributed to visco-elastic or visco-plastic relaxation of surface stresses, the absence of any measurable effect indicated that in-plane stresses alone were not the principal source of the observed toughening effect.

In a recently developed mechanistic model of Case-II sorption [5] it was demonstrated that the presence of an out-of-surface tensile stress should quite significantly enhance the material-misfit-driven elasto-plastic extrusion process of the diluent-laden polymer through the sharp Case-II process front. While such stresses are present in the base of craze tufts that can indeed accelerate plasticization and craze tuft drawing as was indicated in a new diluent-enhanced craze plasticity model [12], this effect too is considered to fall short to explain the dramatic toughening effects observed by Gebizlioglu et al. [6] and by Qin et al. [13] in more expanded recent studies of this same system. Thus, the principal proposition advanced by us [11] and in less direct form by some other investigators earlier [3,14] is that Case-II sorption is enhanced dramatically when a glassy polymer is undergoing large strain plastic flow at the same time as Case-II sorption is occurring. This notion that in active plastic deformation of a glassy polymer the plastic-strain-producing molecular segmental rearrangements can result in a dynamic ‘flow state’ of steady state dilatation and that this could be the source of enhanced diluent conductance is quite natural.

In the present investigation, we demonstrate that this is indeed the case in the Ultem/RDP system, which offers certain distinct advantages that have also permitted us to build on the experience gained in the earlier extensive studies of Case-II diffusion in this system using Rutherford Backscattering Spectroscopy (RBS) to monitor the penetration of the diffusion front [11].

For reasons that we will present, the demonstration of the deformation-enhanced Case-II sorption is best carried out in a setting of so-called limited-supply diffusion that we had used in our earlier study of the Ultem/RDP system

[11]. Nevertheless, since a certain level of more conventional familiarity with Case-II diffusion in this system is necessary, we discuss first experiments carried out in a setting of unlimited diluent supply and in the absence plastic flow.

## 2. Experimental details

### 2.1. Materials

The poly (ether imide) Ultem™ was supplied by the General Electric Co. in pellet, sheet and cylinder forms. The chemical structure is shown in Fig. 1a. Ultem has a high glass transition temperature ( $\sim 215^\circ\text{C}$ ) and is resistant to crazing in a dry environment [13]. Its density at  $20^\circ\text{C}$  is  $1.27\text{ g/cm}^3$ . The diluent used in this experiment is resorcinol bis(diphenyl phosphite) (RDP). This flame-retardant plasticizer, known as Fyrolflex, was supplied by Akzo Chemicals Inc. in the form of a viscous liquid ( $\sim 600\text{ mPa s}$  at  $20^\circ\text{C}$ ). Fig. 1b shows the chemical structure of the RDP compound. Approximately 70% of the material is dimer with a few percent of triphenyl phosphite. The product is non-volatile (vapor pressure  $< 1\text{ mmHg}$  near  $40^\circ\text{C}$ ) and stable up to  $370^\circ\text{C}$ . The density of RDP is  $1.3\text{ g/cm}^3$ . RDP contains the heavy element phosphorous, which is an asset for the RBS experiment described below.

### 2.2. Rutherford backscattering spectroscopy

The ion beam analysis technique employed in this research is RBS, which is sensitive to medium and heavy atomic mass elements. A high energy beam of monoenergetic alpha particles  $4\text{He}^{++}$  of 2 MeV is directed towards the sample.  $\text{He}^{++}$  ions backscattered by nuclei at, or beneath, the polymer surface are collected by an energy-sensitive detector. The detector is connected to a multi-channel analyzer and the particles, which reach the detector are counted as a function of their energy. The energy range of interest, 0–2 MeV, is divided into a number of channels such that each channel spans approximately 2 keV. The information obtained in an experimental RBS spectrum is a result of the effect of the mass of the target nucleus on the energy of the scattered  $\text{He}^{++}$  ion. The energy spectrum is converted readily to a concentration-depth profile for a particular element; in this work, phosphorous concentration is the relevant variable since the RDP plasticizer contains phosphorous. The range of depth probed by RBS, about 1000 nm, is well matched to the concentration profiles developed in our experiments. More detailed discussion of the RBS technique can be found in our earlier publications [11,15,16] and elsewhere [17,18]. The RBS scattering experiments were carried out at the Cambridge Accelerator for Materials Science at Harvard University.

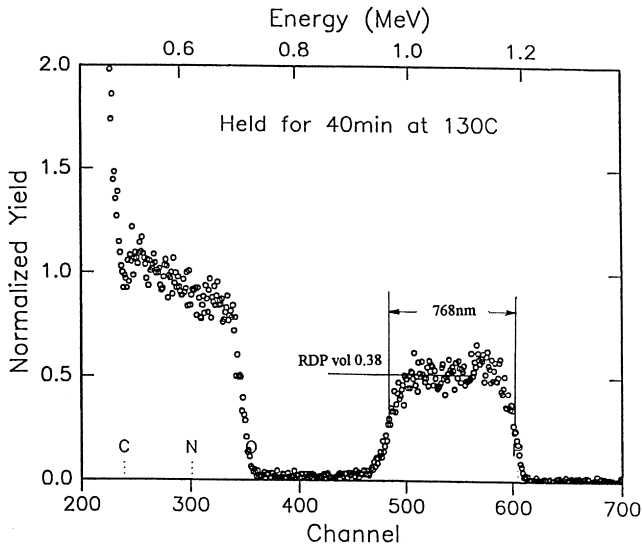


Fig. 2. A typical experimental RBS spectrum of RDP diffusing into Ultem, held for 40 min at 130°C.

### 3. Unlimited-supply diffusion without plastic deformation

#### 3.1. Sample preparation

An Ultem sheet of 1 mm thickness was cut into  $2 \times 2 \text{ cm}^2$  pieces. The samples were placed in an RDP containing thin-walled copper chamber subsequently immersed in a silicon oil bath for a specific period of time. In the temperature range from 120 to 160°C, the RDP in the chamber reaches thermal equilibrium in about 60 s. The period of times used in the diffusion experiments described below was always much longer to eliminate any significant effect of temperature transients on the resulting concentration profiles.

#### 3.2. Results

Fig. 2 shows a typical RBS spectrum in a sample held for 40 min at 130°C in contact with RDP. The plot is shown in terms of channel number (or energy) and detector counts (normalized yield). Backscattered particles at energies between about 1.2 and 0.7 MeV result from collisions with phosphorous atoms below the surface of the sample,

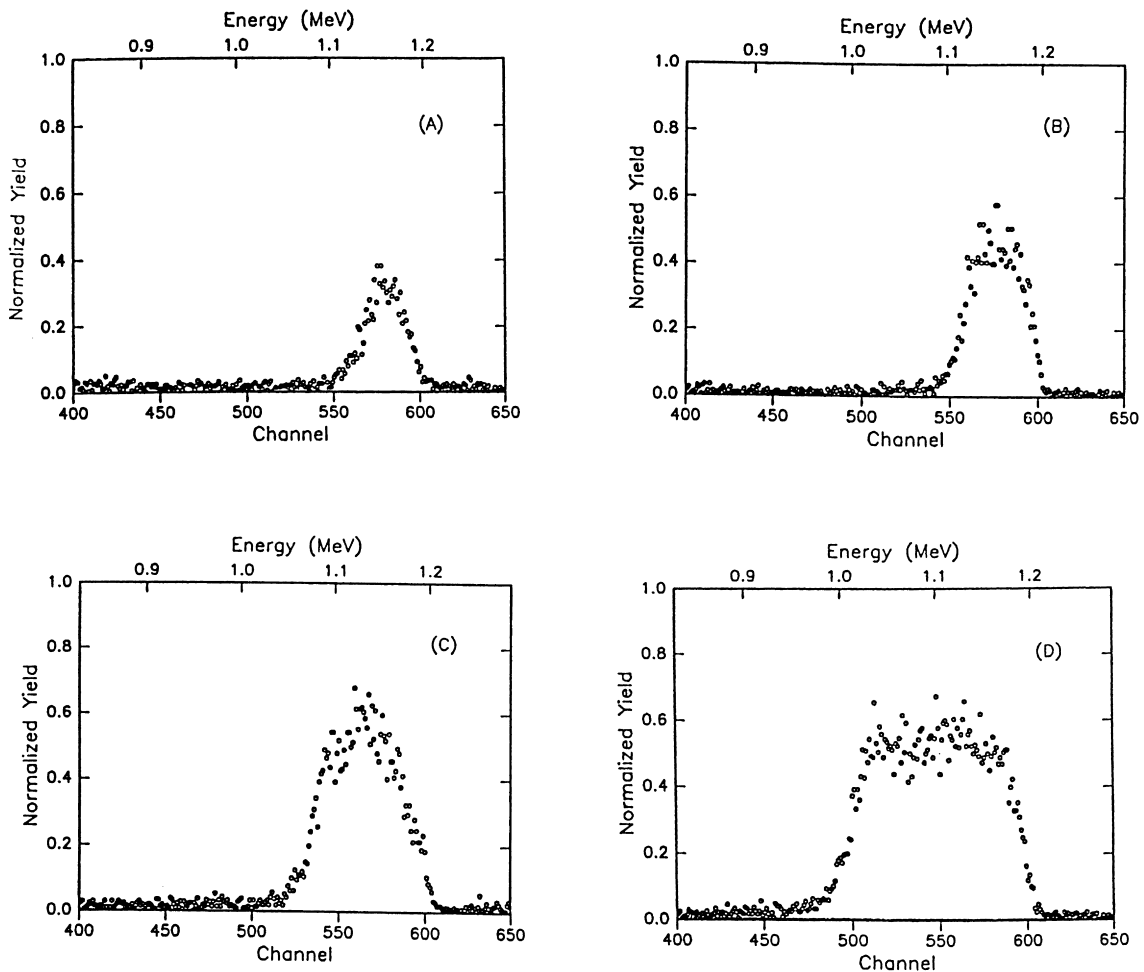


Fig. 3. Experimental RBS spectra showing penetration of RDP fronts in Ultem at 120°C for: (a) 20; (b) 40; (c) 80; (d) 120 min.

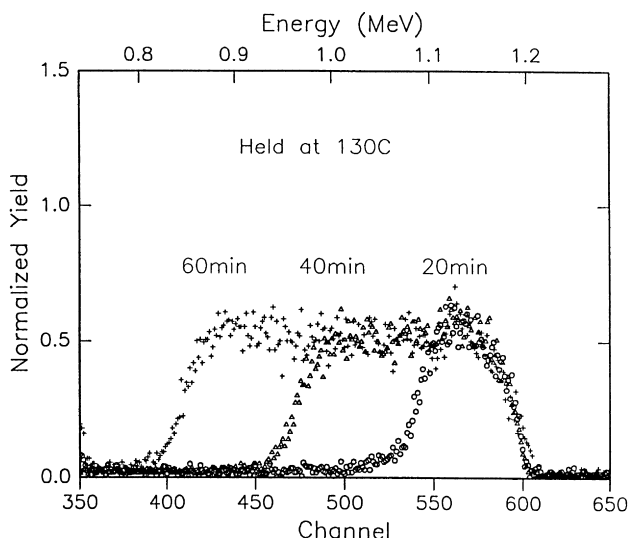


Fig. 4. Case-II diffusion fronts with constant RDP plateau concentrations advancing into Ultem at 130°C with increasing time.

there are no elements before oxygen at the steep rise in the spectrum near 0.7 MeV. The heights of the peaks, can be used to calculate the relative atomic concentrations of the elements at a particular depth [11]. As shown in Fig. 2, RDP moves into Ultem at a constant volume fraction of 0.38 and with a relatively sharp diffusion front, which separates the Ultem into swollen and not swollen material. The swollen layer in Fig. 2 corresponds to a thickness of about 770 nm. This shape of the profile is characteristic of the Case-II diffusion processes mentioned above, and can be used to scale other RBS spectra for penetration depth.

Fig. 3a–d show RBS spectra from Ultem samples held at 120°C for various periods of time in a reservoir of RDP. With increasing time, the diffusion front of RDP moves into Ultem and the RDP concentration behind the diffusion front initially increases, rapidly approaching an approximately constant level. There is an induction period

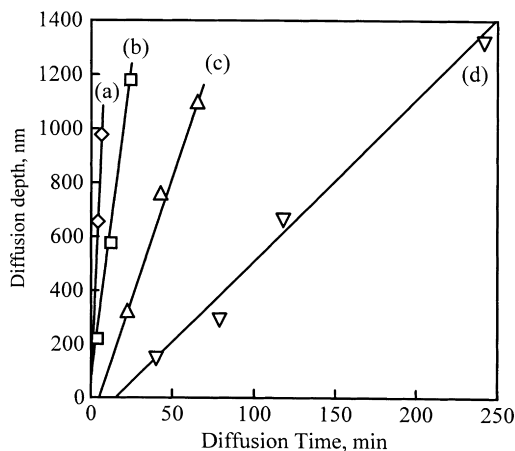


Fig. 5. Diffusion depths of RDP fronts in Ultem with increasing time at: (a) 160; (b) 140; (c) 130; (d) 120°C.

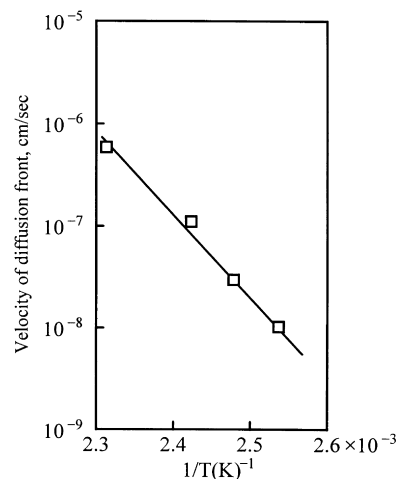


Fig. 6. Temperature dependence of Case-II front velocities of RDP diffusing into Ultem.

required for a Fickian precursor of RDP to form and diffuse into the Ultem before a critical surface concentration is achieved. Once this induction period has elapsed, the Case-II sorption front begins to advance forward and the concentration behind the front remains constant within experimental error.

Fig. 4 shows how the RDP front advances into the Ultem with time at 130°C. Fig. 5 summarizes results of similar experiments showing the advance of Case-II diffusion fronts as a function of time at different temperatures. At 110°C, a Case-II diffusion profile was not observed to form for periods of exposure of up to 10 h, suggesting that the induction time at this temperature is very long. Increasing the temperature to 120°C resulted in the development of a Case-II diffusion front in about 20 min as shown in Fig. 5. RBS spectra of Ultem containing various ranges of RDP penetration: at 120, 130, 140, and 160°C, demonstrated sharp decreases in time for comparable levels of penetration with increasing temperature. The concentration of RDP behind these Case-II fronts showed little sensitivity to temperature, while the values of front velocity  $v$  increased significantly with increasing temperature as must be expected [19]. The slope of the Arrhenius plot of Fig. 6, gives an effective activation enthalpy for  $v$  of about 160 kJ/mol, obtained from such measurements.

Peterlin [20] noted that the Case-II diffusion front is always preceded by a Fickian precursor rising up to a concentration  $\phi_0$  where the swelling induced stresses are sufficient to cause yielding and plastic flow in the plasticized polymer glass. At this point the concentration increases sharply to a higher value  $\phi_\infty$  in the swollen gel corresponding to the equilibrium solubility of the diluent in the gel. Fig. 7 depicts this Case-II concentration profile with Fickian precursor and the very thin nature of the process zone where the final conversion of the polymer from the confined state of diluent-laden plasticized and compressed form into an expanded stress-free gel form occurs. This visco-plastic

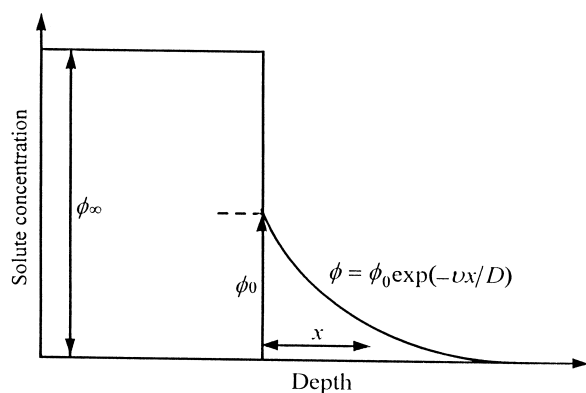


Fig. 7. Schematic rendering of Case-II front advancing toward the right, preceded by a Fickian diffusion front maintaining a self similar profile.

extrusion-like process is discussed in detail in the mechanistic model of Argon et al. [5].

Fickian diffusion precursor profiles are present in the advance of all Case-II fronts. Their steady state forms of diluent concentration has been predicted by Crank [21,22] and specifically determined by Peterlin [20] and can be given as:

$$\varphi(x) = \varphi_0 \exp(-vx/D) \quad (1)$$

where  $v$  is the front velocity,  $x$  the distance ahead of the moving front and  $D$  the diffusion constant of the diluent in the polymer glass ahead of the front.

The forms of the RBS data are simulated with the aid of a so-called RUMP software package developed by Doolittle et al. [23]. Given the parameters of the experimental configuration and the physical and chemical properties of the species in the sample, the program performs iterative fits to get the best least squares functional description of the experimental data. As shown in Fig. 8, the simulated RBS

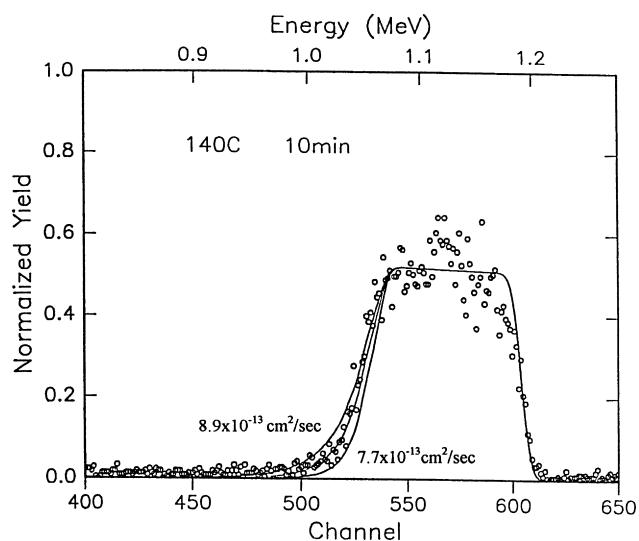


Fig. 8. An RBS spectrum fitted by a simulated spectrum generated by a RUMP software program: for a measured front velocity of  $1.06 \times 10^{-7}$  cm/s with a diffusion constant of  $8.4 \times 10^{-13}$  cm<sup>2</sup>/s at 140°C. Two other trials with diffusion constants of  $8.9 \times 10^{-13}$  cm<sup>2</sup>/s and  $7.7 \times 10^{-13}$  cm<sup>2</sup>/s show the sensitivity of the fit to the chosen diffusion constant.

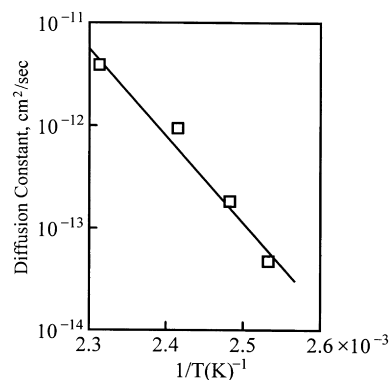


Fig. 9. Temperature dependence of diffusion constants of RDP into Ultem determined from the best fits to the shapes of the Fickian precursors of the measured RDP distributions at the Case-II fronts.

spectra have significant sensitivity to the choice of the value  $D$  of the Fickian diffusion constant. Fig. 9 shows the best-fit values of the diffusion constant  $D$  of RDP in Ultem vs. the reciprocal of the absolute temperature. The slope of the plot corresponds to an activation energy of about 150 kJ/mol, somewhat lower than the value obtained from the temperature dependence of the front velocity given in Fig. 6. This activation energy compares well with activation energies of diffusion of photo-reactive dye molecules of a variety of sizes into glassy polymers such as PS, PES, PMMA, PEMA and PC where the Arrhenian tracer diffusion activation energies ranged from a low of 90 to a high of 220 kJ/mol, [26]. The difference between the two activation energies results from the fact that the velocity of the Case-II front combines the kinetics of both diffusion and plastic flow at the Case-II process front [5].<sup>2</sup>

#### 4. Limited-supply diffusion without and with plastic deformation

##### 4.1. Sample preparation

Both Ultem sheets and Ultem rods have been used to study limited-supply diffusion of RDP with the rods being used in the experiments of concurrent deformation and diffusion. Ultem sheets of 1 mm thickness were cut into  $2 \times 2$  cm<sup>2</sup>, cleaned with detergent solution and then dried in a vacuum oven at room temperature. Mixtures of Ultem and RDP (80% by weight RDP) were deposited on clean glass slides via spin coating from an anisole solution. This

<sup>2</sup> The recent mechanistic model of Case-II diffusion of Argon et al. [5] gives the activation energy governing the advance of the Case-II front as the mean of the activation energies for Fickian diffusion of the diluent and that for the plastic flow of the polymer. While the information given in Fig. 11 is incomplete to fix the value of the latter, for a reasonable pre-exponential factor of  $10^{10}$  s<sup>-1</sup> in the strain rate expression an activation energy of about 170 kJ/mol for plastic flow is obtained, which gives an average of 160 kJ/mol for the activation energy for the motion of the Case-II front that would explain the different measurements quite well.

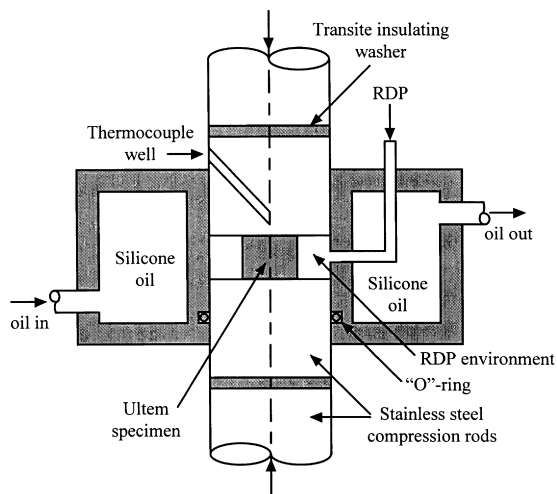


Fig. 10. Sketch of the experimental arrangement for diffusional penetration of RDP at different temperatures into Ultem undergoing concurrent plastic flow.

method produces homogeneous films as demonstrated by transmission electron microscopy [11]. The blended film was floated-off the glass slide onto the surface of a distilled water bath and picked up with the Ultem sheets. The coated Ultem sheets were then dried in a vacuum oven overnight at room temperature, placed in a nitrogen filled thin-walled copper chamber, and subsequently immersed in a silicone oil bath at a given temperature for a desired time for the conduct of the diffusion experiments without deformation. In addition, an alternative method was also used to produce the finite supply layers of the diluents. In this method, Ultem sheets were placed in RDP to allow the RDP to penetrate for a given length of time at a selected temperature to create a diluent-rich surface layer. The plasticized layer on the Ultem surface has then served as the supply layer in subsequent experiments.

#### 4.2. Apparatus for simultaneous diffusion and plastic deformation

A series of early trial experiments demonstrated dramatically that while Ultem is craze resistant in neutral environments, it undergoes rapid and extensive crazing followed by fracture, if stressed in an environment of liquid RDP at temperatures at or above room temperature. Since the sought after synergistic coupling of Case-II diffusion was with a plastically deforming polymer and that the crucial dilated flow state should be achievable by plastic flow in compression as well as in any other form, the combined experiment was performed under a state of compression flow to eliminate undesirable crazing effects.

A sketch of the experimental arrangement that was used in these experiments is presented in Fig. 10. The cylindrical Ultem compression samples were surrounded by an RDP liquid environment maintained at a given temperature by means of a special annular heating jacket fitting snugly

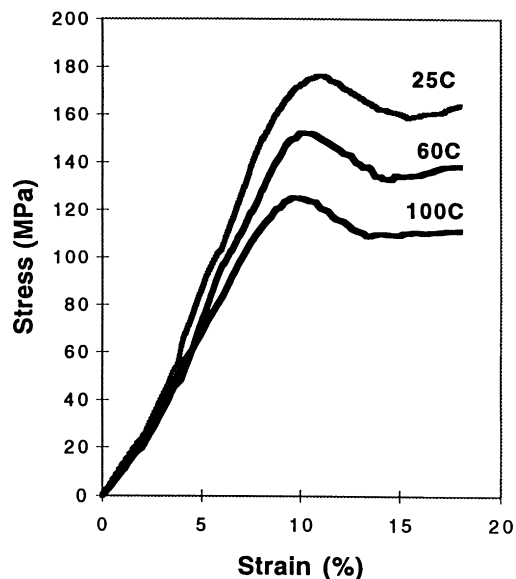


Fig. 11. Compression stress strain curves of Ultem at a strain rate of  $10^{-4} \text{ s}^{-1}$  at three different temperatures.

around the compression grips and delineating the active specimen chamber. The temperature in the heating jacket was maintained constant by means of heated silicone oil, that was part of an external circulating system. The temperature of one of the compression grips was measured close to the specimen by a specially placed thermocouple. The time constant for reaching thermal equilibrium in the specimen, typically of the order of 40 min, was governed by the thermal inertia of the stainless steel compression grips rather than that of the specimens.

The compression samples contained axial flats that were polished meticulously by metallographic techniques with diamond grit, starting with  $3 \mu\text{m}$  particles and ending up with  $0.05 \mu\text{m}$  particles. Such polishing was necessary to suppress spurious crazing that would otherwise develop even from deformation-induced surface roughening.

For limited-supply diffusion experiments, the required thin homogeneous films of 80%RDP/20%Ultem, were deposited on the polished flats as described above. In these limited-supply diffusion experiments, there was no RDP present in the compression chamber. The specimen was compressed in air at temperature maintained by the same heating jacket described above.

To reduce friction between compression surfaces of the apparatus and the ends of the cylinders, shallow circumferential grooves were cut into both ends of the samples. The grooves trap graphite powder that lubricates effectively the compression surfaces and minimizes plastic barreling. This technique that had been used effectively by Brown et al. [24] for large strain plastic compression of Al and Fe specimens has also minimized barreling of the Ultem in the present experiments. The compression experiments were performed on an Instron Model 4505 machine. Fig. 11 shows compression stress–strain curves of uncoated Ultem at different

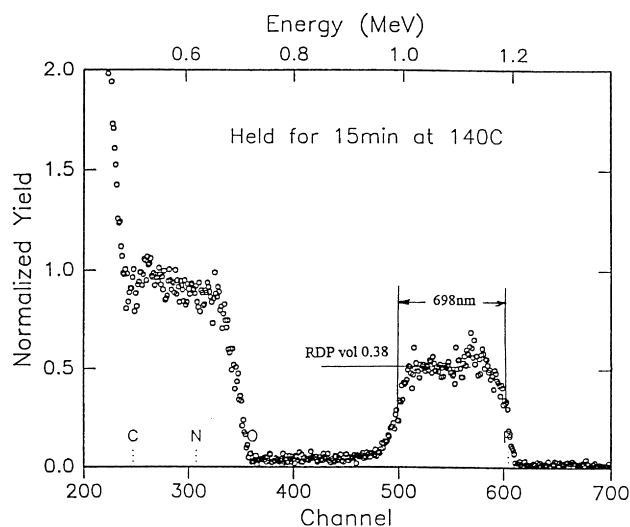


Fig. 12. A typical RBS spectrum of limited-supply diffusion for a sample held at 140°C for 15 min. Compare with the result of the RBS spectrum of Fig. 2, obtained with unlimited diluent supply.

temperatures at a strain rate of  $10^{-4} \text{ s}^{-1}$  based on initial specimen geometry. The curves show the intrinsic decrease of the plastic resistance with temperature at constant strain rate. The pronounced yield drops indicate that the Ultem started deforming from a well aged state.

#### 4.3. Limited-supply diffusion without plastic deformation

Fig. 12 shows a typical RBS spectrum from a one step limited-supply diffusion experiment in the absence of deformation. The sample was held for 15 min at 140°C. It is clear that the limited-supply layer of RDP, placed on the surface, has moved into the initially pure Ultem substrate and has created a sharp diffusion front separating the swollen material behind the front from the not swollen material ahead of it. A Fickian precursor front preceding the Case-II front is discernable. The concentration of RDP at a level of 0.38 is constant in the plasticized layer, and the appearance of the diluent concentration profile in this one step experiment is identical to the profile of the unlimited-supply case of Fig. 2. Below  $T_g$  all limited-supply diffusion profiles have appearances similar to that of Fig. 12.

Fig. 13 shows the RDP diffusion front moving into the Ultem under the limited-supply boundary condition. In this experiment, the supply layer was obtained by the second procedure in which RDP at high concentration in contact with the surface was allowed to diffuse into the Ultem for 20 min at 130°C to achieve a volume fraction of 0.38. This represents the first, highest concentration contour in Fig. 13. When the diffusion front moves deeper into the specimen in three further steps at 130°C in hold times of 30, 60 and 80 min, the other concentration profiles develop. Since the total RDP concentration remains constant, the concentrations in these subsequent profiles decrease systematically as the overall quantity of the integrated RDP remains

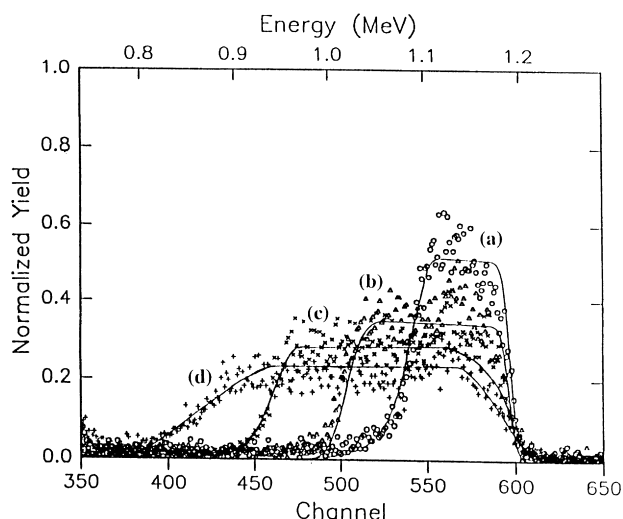


Fig. 13. Leveling-down of RDP concentrations by Case-II front penetrations into Ultem at 130°C in a limited-supply diffusion experiment showing the advance of the Case-II profile with increasing time (in min): (a) 20; (b) 30; (c) 60; (d) 80. Total integrated RDP concentration of all profiles should be the same.

constant. Moreover, since the RDP concentration in the profiles decrease the front advances with decreasing velocity [5,11].

#### 4.4. Limited-supply diffusion with concurrent plastic flow

At 215°C, the  $T_g$  of Ultem, a completely different picture emerges in the diffusion of RDP into the Ultem, when compared with the behavior well below  $T_g$  such as at 130°C shown in Fig. 13. As Fig. 14 shows, the diffusion profile is altered very substantially. The peak height of the phosphorous signal decreases rapidly with time. The characteristic sharp diffusion fronts and the constant concentrations of RDP behind the fronts no longer exist as is seen in Fig. 14.<sup>3</sup> At  $T_g$ , the initial concentration of RDP drops rapidly to very low values by draining into the background since the resistance to diluent penetration in the dilated molecular structure of  $T_g$  is now dramatically lower. Moreover, the finite levels of plastic resistance of the unmodified polymer that are instrumental in the fashioning of the sharp Case-II front are also no longer present.

Fig. 15 shows the RBS profiles from an Ultem Specimen, bearing an RDP containing film on its flats, being deformed plastically at a constant compression rate of roughly  $10^{-4} \text{ s}^{-1}$  at 113°C, about 102°C below  $T_g$ . The different profiles are for different levels of plastic strain  $\epsilon^p$  at given levels of elapsed time  $t_d(t_d/\epsilon^p)$ . The increasing levels of plastic strain, with negligible strain hardening, merely

<sup>3</sup> The dotted curve represents the initial RDP peak. Maintaining this peak unaltered in the experiment at or above  $T_g$  is not readily possible as it disperses during the relatively long periods of heating the cylindrical samples. The shape of this peak should be the same as the initial peak shown in Fig. 15.

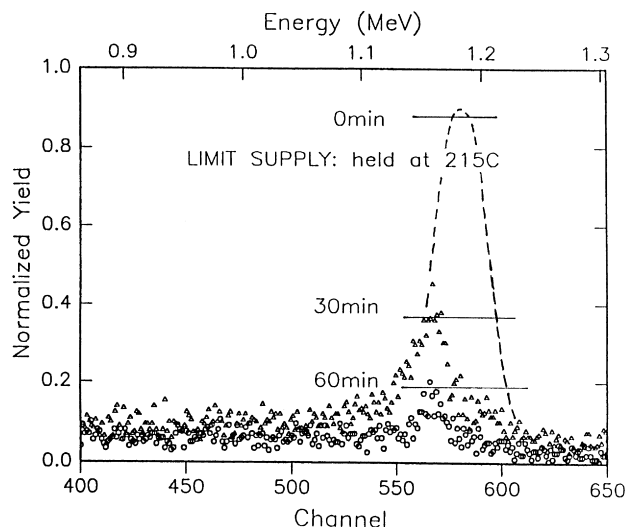


Fig. 14. RBS spectra of RDP concentrations showing leveling-down at 215°C with increasing hold times, from an initial limited-supply layer of RDP.

serve to maintain a steady state of flow dilatation during which diffusion can progress with increasing time. We recall from Section 3.2 that at 110°C no diluent penetration occurred into Ultem in 10 h when deformation was absent. The observed diffusion behavior of Fig. 15 looks radically different from that shown in Fig. 13 for 130°C without deformation, but instead looks nearly identical to the changing diluent uptake profiles shown in Fig. 14 for 215°C. The peaks of phosphorous concentration decrease in the same manner by monotonic draining-away of the RDP diluent into the interior material maintained at the dilated flow state by plastic flow rather than by temperature as was the case at 215°C, without deformation.

## 5. Discussion

Limited-supply diffusion of the RDP plasticizer in the glassy Ultem polymer represents an unusually revealing way to demonstrate non-Fickian diffusion of plasticizer in a glassy polymer. In the limited-supply condition, the diffusion front does not move linearly with time at fixed temperature. Conservation of mass of diluent requires the concentration of RDP in the plasticized zone to decrease systematically with time and diffusion depth. As pointed out by Nealey et al. [11], the properties of the material behind the diffusion front change with time and penetration depth, continuously altering the local driving forces that advance the diffusion front. Because the diffusion front velocity is not independent of time, only instantaneous front velocities can be calculated as a function of concentration.

Increasing the temperature to  $T_g$ , and above, eliminates the confining nature of the bulk polymer glass by molecularly dilating it and eliminating its plastic resistance. The material misfit due to the uptake of the diluent can now be

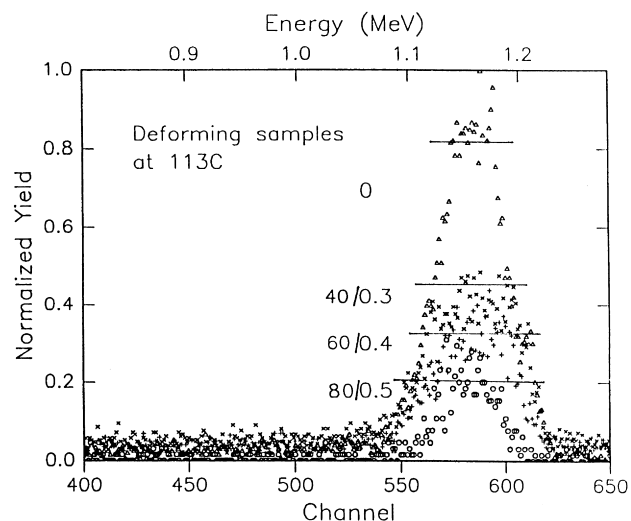


Fig. 15. RBS spectra of RDP concentration showing leveling-down at 113°C from an initial limited-supply layer of RDP while the Ultem was undergoing concurrent plastic flow at a strain rate of  $10^{-4} \text{ s}^{-1}$ . The decreasing levels of peak diluent concentration are given for elapsed times  $t_d$  required to reach plastic strains  $\epsilon^p(t_d/\epsilon^p)$ .

accommodated with little resistance and the sharp Case-II fronts become leveled-down completely [5]. Mills et al. [19] have speculated that the critical concentration at the back edge of the Fickian precursor front is dictated by the amount of diluent to match the  $T_g$  of the mixture with the ambient temperature  $T$ . Thus, when  $T$  approaches  $T_g$  of the undiluted polymer, the limited-supply diffusion front can advance at very low diluent concentrations. Fig. 15 shows this effect. The initial surface layer of RDP-enriched polymer disappears with time, as the concentration of the RDP drains rapidly into the thermally dilated bulk where it remains at a very low level. The required material balance (constant area under the spectrum as in Fig. 13) cannot be seen in Fig. 14 because at the elevated temperature of the experiments, the diluent has drained rapidly into the sample beyond the depth resolution of the RBS experiment.

The striking similarity between Figs. 14 and 15 suggests that active plastic flow well below  $T_g$  (here, at 113°C, roughly 100°C below the  $T_g$  of Ultem) brings the material to a *mechanically dilated flow state* having a steady state structure that is effectively the same as the material at  $T_g$ . This dilated flow state requires active plastic deformation for its maintenance. Cessation of deformation returns the material to a compacted inactive state characteristic of the low temperature behavior in which diluent diffusion drops to negligible levels (at 113°C).

It is attractive to view the plastic-flow-induced increase of the diluent conductance in the glassy polymer as an apparent increase in the diffusion constant of the diluent in the glassy polymer at the low temperature of plastic deformation. Based on the measured diffusion constant of RDP in Ultem and on the notion of the structural correspondence of the mechanically dilated flow state at 113°C and the



thermally dilated state at  $T_g$  at 215°C this would amount to an increase in the diffusion constant by a factor of  $1.9 \times 10^4$  in the present case. Such interpretations, however, require caution since the increased conductance is only partially a consequence of a structural correspondence, but requires also ready mobility of the diluent molecule in the mechanically dilated structure. This would systematically decrease in proportion to the decreasing fluidity of the diluent with decreasing temperature. This effect was encountered by Qin et al. [13] in the toughening by craze plasticity of PS with a series of PB diluents of 3 kg/mol, but with several different isomer forms having fluidity ranging over two orders of magnitude. The diluents with the highest fluidity continued to be effective to lower temperatures than those with lower fluidity [12].

The results presented in Fig. 15 resolve quite well the apparent difficulties encountered in the earlier experiments of Nealey et al. [11] where the simple application of a biaxial tensile or compressive stress at substantial fractions of the flow stress (but resulting in no flow) had produced no important effects, with the Case-II diffusion process remaining virtually unaltered. On the other hand the source of the accelerated crazing response in the PS/PB blends [6–10] where active plastic drawing occurred at the base of the craze matter tufts becomes quite clear. Parenthetically, these observations explain also why the limited-supply diffusion experiment has been very successful in demonstrating the synergistic effect and why the unlimited-supply diffusion experiments with concurrent plastic flow in the presence of the RDP diluent in the special chamber were generally less successful. In the latter experiments, the plastic flow produces a dilated flow state with high diluent conductance where, as a result, with rapid diluent uptake no significant characteristic Case-II profiles of the type shown in Fig. 13 develop, and the diluent penetration becomes difficult to demonstrate.

In summary, our *limited-supply diffusion* experiment has demonstrated conclusively that diffusional conductance of diluents into glassy polymers is enhanced dramatically by orders of magnitude if the glassy polymer is undergoing plastic flow. The only other observation resembling to ours comes from an experimental study of Windle [25] exploring the effect of prior plastic deformation on subsequent Case-II sorption rates, where it was found that the effect of prior plastic deformation of PMMA, whether produced in tension or compression at room temperature, was an increase in the diluent (methanol) penetration rate by a factor of up to five. In addition, significantly higher penetration rates were measured perpendicular to the direction of principal extension than parallel to it—which too was larger than that in the not deformed sample. Clearly, these observations are in full accord with our study, which, however, demonstrates clearly the far more dramatic effect of a flow state rather than the residual effect after flow.

It is interesting to note that there has been a long standing realization in the polymer literature that there is some

relationship between the process of plastic flow and the glass transition where, however, nearly in every case the cause/effect relationship had been inverted by propositions that application of stress brings the material to its glass transition, which then provides the required mobility that permits plastic flow. We have demonstrated the true form of this relationship as being one in which plastic flow produces a mechanically dilated flow state that resembles closely the purely thermally dilated state at  $T_g$  with its well recognized free volume. In both cases the resulting segmental level dilatations permit rapid diluent uptake and conductance.

## Acknowledgements

This research was supported by the MRSEC Program of NSF through the MIT Center for Materials Science and Engineering under Grant DMR-94-00334 and was importantly aided by two successive Aid to Education Grants of the DuPont Co. of Wilmington Delaware. We acknowledge a number of useful discussions with Prof Paul Nealey of the University of Wisconsin and the help of John Chervinsky of the Cambridge Accelerator for Materials Science in the conduct of the RBS measurements. Finally, we are grateful to Prof Alan Windle for bringing to our attention his experiments on the effects of prior plastic deformation [25].

## References

- [1] Alfrey T, Gurnee EF, Lloyd WG. *J Polymer Sci* 1966;12:249.
- [2] Lasky RC, Kramer EJ, Hui C-Y. *Polymer* 1988;29:673.
- [3] Gall TP, Lasky RC, Kramer EJ. *Polymer* 1990;31:1491.
- [4] Thomas NL, Windle AH. *Polymer* 1982;23:529.
- [5] Argon AS, Cohen RE, Patel AC. *Polymer* 1999;40:6991.
- [6] Gebizlioglu OS, Beckham WH, Argon AS, Cohen RE, Brown HR. *Macromolecules* 1990;23:3968.
- [7] Piorkowska E, Argon AS, Cohen RE. *Polymer* 1993;34:4435.
- [8] Brown HR, Argon AS, Cohen RE, Gebizlioglu OS, Kramer EJ. *Macromolecules* 1989;22:1002.
- [9] Spiegelberg SH, Argon AS, Cohen RE. *J Appl Polym Sci* 1995;58:85.
- [10] Spiegelberg SH, Cohen RE. *Polymeric materials encyclopedia* 1996;4:2798.
- [11] Nealey PF, Cohen RE, Argon AS. *Polymer* 1995;36:3687.
- [12] Argon AS. *J Appl Polym Sci* 1999;72:13.
- [13] Qin J, Argon AS, Cohen RE. *J Appl Polym Sci* 1999;71:1469.
- [14] Harmon JP, Li JCM, Samboh L. *J Polym Sci, Polym Phys Ed* 1987;25:3215.
- [15] Nealey PF, Cohen RE, Argon AS. *Macromolecules* 1993;26:1287.
- [16] Nealey PF, Cohen RE, Argon AS. *Macromolecules* 1994;27:4193.
- [17] Feldman LC, Meyer JW. *Fundamentals of surface thin film analysis*. New York: Elsevier, 1986.
- [18] Chu WR, Mayer JW, Nicolet MA. *Backscattering spectroscopy*. New York: Academic Press, 1978.
- [19] Mills PJ, Palmstrom CJ, Kramer EJ. *J Mater Sci* 1986;21:1479.
- [20] Peterlin A. *J Polym Phys* 1965;3:1083.
- [21] Crank JJ. *Polym Sci* 1953;11:151.
- [22] Doolittle LR. *Nucl Instrum Methods* 1985;9:344.
- [23] Doolittle LR. *Nucl Instrum Methods* 1986;15:227.
- [24] Brown SB, Kim KH, Anand L. *Int J Plast* 1989;5:95.
- [25] Windle AH. *J Membr Sci* 1984;18:87.
- [26] Ehlich D, Sillescu H. *Macromolecules* 1990;23:1600.